International Journal of Earth, Energy and Environmental Sciences
ISSN: 2517-942X
Vol:10, No:4, 2016

Probabilistic Simulation of Triaxial Undrained Cyclic Behavior of Soils

Arezoo Sadrinezhad, Kallol Sett, S. I. Hariharan

Abstract—In this paper, a probabilistic framework based on Fokker-Planck-Kolmogorov (FPK) approach has been applied to simulate triaxial cyclic constitutive behavior of uncertain soils. The framework builds upon previous work of the writers, and it has been extended for cyclic probabilistic simulation of triaxial undrained behavior of soils. von Mises elastic-perfectly plastic material model is considered. It is shown that by using probabilistic framework, some of the most important aspects of soil behavior under cyclic loading can be captured even with a simple elastic-perfectly plastic constitutive model.

Keywords—Elasto-plasticity, uncertainty, soils, Fokker-Planck equation, Fourier Spectral method, Finite Difference method.

I. Introduction

THE cyclic behavior of soils plays an important role in various engineering problems. For instance, in the field of geotechnical earthquake engineering, evaluation of the seismic ground motion, liquefaction potential, etc., can be strongly influenced by the cyclic behavior of soils. Therefore, in recent years, the response of soils to cyclic loading has received considerable attention in geotechnical earthquake engineering.

Researchers have developed different advanced deterministic constitutive models within the framework of Critical State Soil Mechanics (CSSM) in order to simulate complex soil behavior more realistically [1]. One of these models is the Dafalias-Manzari model (DM04) which is capable of predicting monotonic undrained and drained behavior of soils [2]. However, DM04 model is unable to capture some of the aspects of soil behavior under undrained cyclic loading (e.g., effective stress reduction and modulus degradation) [3].

In order to overcome the shortcomings of DM04, Boulanger and Ziotopulou proposed a Plasticity Model for Sand (PM4Sand) based on the DM04 which is capable of predicting soil behavior under cyclic loading. However, this model uses 22 different parameters to simulate constitutive soil behavior of soils [4]. Since in geotechnical engineering practice, advanced laboratory tests are rarely performed, it is important to find other models to simulate cyclic constitutive behavior of soils using less number of parameters.

In order to simulate soil behavior more realistically, considering the inherent uncertainties in soil properties is necessary. These uncertainties are due to the inherent variability of soil deposits [5], [6], measurement uncertainties [7]–[10], and transformation relation uncertainties [11]. In order to take these uncertainties into account, probabilistic techniques are required. However, existing probabilistic models, such as Monte Carlo Simulation (MCS) technique [12]–[16] and perturbation method [17] have limitations in modeling of nonlinear problems. MCS technique is computationally very expensive for a nonlinear problem with multiple uncertain material properties. On the other hand, perturbation technique is limited to problems with small coefficient of variations (COVs) (less than 20%) [18]. Given that, for some soil properties COV is greater than 70%, perturbation techniques cannot be applied. To overcome these drawbacks, Sett, Unutmaz et al. [19], [20] developed a probabilistic model based on FPK approach [21] to simulate one-dimensional cyclic behavior of soils probabilistically. They observed that by taking soil uncertainties into account, even with a simple von Mises elastic-perfectly plastic model, which requires only two soil parameters (elastic shear modulus (G) and undrained shear strength (s_u)), a realistic cyclic material behavior can be obtained. However, the developed FPK based probabilistic framework for cyclic constitutive modeling of soils is a one-dimensional framework which cannot be used for simulation of real world problems. Therefore, the first aim of this study is to extend the one-dimensional FPK based framework for constitutive modeling of soils to a multi-dimensional FPK framework. Moreover, the existing one-dimensional FPK based framework utilizes the Finite Difference (FD) technique for solving the governing FPK equation which is not computationally efficient for a multi-dimensional problem. Thus, the second goal of this study is to develop a computationally efficient algorithm for solving the governing multivariate FPK equation.

II. Mathematical Forms of the Governing FPK Equations

The general constitutive rate equation for an uncertain, elastic- perfectly plastic material can be written in the probability density space as [19], [22]–[25]:

$$\frac{\partial P(\boldsymbol{\sigma},t)}{\partial t} = - \frac{\partial}{\partial \sigma_{mn}}\left[N^{\sigma^{eq}}_{(1)_{mn}}(\boldsymbol{\sigma};t)\ P(\boldsymbol{\sigma},t)\right] + \frac{\partial^2}{\partial \sigma_{mn}\partial \sigma_{ab}}\left[N^{\sigma^{eq}}_{(2)_{mnab}}(\boldsymbol{\sigma};t)\ P(\boldsymbol{\sigma},t)\right] \quad (1)$$

where $\boldsymbol{\sigma}$ is the stress tensor, $\{\sigma_{11},\sigma_{22},\sigma_{33},\sigma_{12},\sigma_{23},\sigma_{31}\}$, P is the joint probability density of the components of the stress tensor, t is the pseudo time of the constitutive rate

A. Sadrinezhad is with the California State University, Fresno, CA 93740 USA (corresponding author to provide phone: 559-278-1657; fax: 559-278-7002; e-mail: asadrinezhad@csufresno.edu).

K. Sett is with Department of Civil, Structural and Environmental Engineering, University at Buffalo, The State University of New York, Buffalo, NY 14260 USA (e-mail: kallolse@buffalo.edu).

S. I. Hariharan is with the Department of Electrical and Computer Engineering, University of Akron, Akron, OH 44325 USA (e-mail: hari@uakron.edu).

equation, $N^{\sigma^{eq}}_{(1)_{mn}}$ and $N^{\sigma^{eq}}_{(2)_{mnab}}$ are the equivalent advection and diffusion coefficients, respectively, of the stress FPK PDE. Note that the indices, m, n, a, and b vary from 1 to 3.

The mathematical forms of the equivalent advection and diffusion coefficients of the FKP PDEs, $N^{\sigma^{eq}}_{(1)_{mn}}$, and $N^{\sigma^{eq}}_{(2)_{mnab}}$, for a constitutive model based on the classical plasticity theory, may be expressed as:

$$\begin{aligned} N^{\sigma^{eq}}_{(1)_{mn}}(\boldsymbol{\sigma};t) &= Pr\left[F<0\right](\boldsymbol{\sigma})N^{\sigma^{el}}_{(1)_{mn}} \\ &+ \left\{1-Pr\left[F<0\right](\boldsymbol{\sigma})\right\}N^{\sigma^{pl}}_{(1)_{mn}}(\boldsymbol{\sigma},;t) \end{aligned} \tag{2}$$

$$\begin{aligned} N^{\sigma^{eq}}_{(2)_{mnab}}(\boldsymbol{\sigma};t) &= Pr\left[F<0\right](\boldsymbol{\sigma})N^{\sigma^{el}}_{(2)_{mnab}}(t) \\ &+ \left\{1-Pr\left[F<0\right](\boldsymbol{\sigma})\right\}N^{\sigma^{pl}}_{(2)_{mnab}}(\boldsymbol{\sigma};t) \end{aligned} \tag{3}$$

where F is the yield function which is a function of $\boldsymbol{\sigma}$, $Pr\left[F<0\right]$ is the probability that material is elastic (stresses are inside the yield surface), $1-Pr\left[F<0\right]$ is the probability that material is plastic (stresses are on the yield surface), $N^{\sigma^{el}}_{(1)_{mn}}$ and $N^{\sigma^{el}}_{(2)_{mnab}}$ are the elastic advection and diffusion coefficients, $N^{\sigma^{pl}}_{(1)_{mn}}$ and $N^{\sigma^{pl}}_{(2)_{mnab}}$ are the plastic advection and diffusion coefficients. The elastic and plastic advection and diffusion coefficients may be mathematically expressed as:

$$N^{\sigma^{el}}_{(1)_{mn}} = \left\langle D^{el}_{mnrs}\dot{\epsilon}_{rs}\right\rangle \tag{4}$$

$$N^{\sigma^{el}}_{(2)_{mnab}}(t) = t\ \ Cov\left[D^{el}_{mnrs}\dot{\epsilon}_{rs}; D^{el}_{abcd}\dot{\epsilon}_{cd}\right] \tag{5}$$

$$\begin{aligned} N^{\sigma^{pl}}_{(1)_{mn}}(\boldsymbol{\sigma};t) &= \left\langle D^{pl}_{mnrs}(\boldsymbol{\sigma};t)\dot{\epsilon}_{rs}\right\rangle + \\ &\int_0^t d\tau Cov_0\left[\frac{\partial}{\partial\sigma_{ab}}\left\{D^{pl}_{mnrs}(\boldsymbol{\sigma};t)\dot{\epsilon}_{rs}\right\}; \right. \\ &\left. D^{pl}_{abcd}(\boldsymbol{\sigma};t-\tau)\dot{\epsilon}_{cd}\right] \end{aligned} \tag{6}$$

$$\begin{aligned} &N^{\sigma^{pl}}_{(2)_{mnab}}(\boldsymbol{\sigma};t) = \\ &\int_0^t d\tau Cov_0\left[D^{pl}_{mnrs}(\boldsymbol{\sigma};t)\dot{\epsilon}_{rs}; D^{pl}_{abcd}(\boldsymbol{\sigma};t-\tau)\dot{\epsilon}_{cd}\right] \end{aligned} \tag{7}$$

where D^{el}_{mnrs} is the elastic modulus, D^{pl}_{mnrs} is the plastic modulus, and $\dot{\epsilon}_{rs}$ is the rate of strain. In the above equations, $\langle\cdot\rangle$ denotes expectation operation, $Cov\left[\cdot\right]$ denotes covariance operation, $Cov_0\left[\cdot\right]$ denotes time-ordered covariance operation, and τ is the lag (pseudo) time. The elastic and plastic moduli, D^{el}_{ijkl} and D^{pl}_{ijkl}, assuming material isotropy, may be expressed as [26]:

$$D^{el}_{ijkl} = \frac{E}{2(1+\nu)}\left[\frac{2\nu}{1-2\nu}\delta_{ij}\delta_{kl}+\delta_{ik}\delta_{jl}+\delta_{il}\delta_{jk}\right] \tag{8}$$

$$D^{pl}_{ijkl}(\boldsymbol{\sigma};t) = D^{el}_{ijkl} - \frac{\frac{\partial F}{\partial\sigma_{ot}}D^{el}_{ijot}D^{el}_{pqkl}\frac{\partial U}{\partial\sigma_{pq}}}{\frac{\partial U}{\partial\sigma_{ab}}D^{el}_{abcd}\frac{\partial F}{\partial\sigma_{cd}}} \tag{9}$$

where E is the Young's modulus, ν is the Poisson's ratio, F is the yield function, U is the plastic potential function, and δ_{ij} is the Kronecker delta.

A. Initial and Boundary Conditions

Initial conditions for the governing FPK equation (1) could be deterministic or probabilistic. In this study, a deterministic initial condition which can be mathematically represented by a (multidimensional) Dirac delta function is assumed. Regarding the boundary conditions, a reflecting boundary condition is considered. Mathematically, this boundary condition can be achieved by considering zero probability current, ζ, at any point. Therefore, the boundary conditions of (1) can be written as:

$$\begin{aligned} &\zeta_{mn}(\boldsymbol{\sigma},t)|_{at\ boundaries} = \left\{N^{\sigma^{eq}}_{(1)_{mn}}(\boldsymbol{\sigma};t)\ P(\boldsymbol{\sigma},t) - \right. \\ &\left.\frac{\partial}{\partial\sigma_{ab}}\left[N^{\sigma^{eq}}_{(2)_{mnab}}(\boldsymbol{\sigma};t)\ P(\boldsymbol{\sigma},t)\right]\right\}\Big|_{at\ boundaries} = 0 \end{aligned} \tag{10}$$

In the following the above general forms of the FPK equation will be specialized for simulating the unconsolidated undrained cyclic triaxial compression Test in geotechnical engineering. Note that the von Mises elastic-perfectly plastic model is considered.

III. Unconsolidated Undrained Triaxial Compression Test

Triaxial compression test is a standard test in geotechnical engineering [27]. In this test, first, an isotropic compression is applied on a cylindrical soil specimen and then the specimen is sheared by gradually increasing the axial strain, ϵ_1, while the confining pressure σ_3 is remained constant (σ_2 = σ_3). Triaxial compression test can be performed under drained and undrained conditions. Under the drained condition, water is allowed to drain and the excess pore water pressure dissipates. On the other hand, under the undrained condition, water is not allowed to escape the pores which results in an increase in the pore water pressure. However, the change in the volumetric strain, $d\epsilon_1+d\epsilon_2+d\epsilon_3$, is zero during shearing.

In this study, an unconsolidated undrained triaxial compression test is simulated. By assuming a von Mises elastic-perfectly plastic model, the FPK equation may be written in the principal stress space as:

$$\begin{aligned} \frac{\partial P(\boldsymbol{\sigma},t)}{\partial t} &= -\ \frac{\partial}{\partial\sigma_r}\left[N^{\sigma^{eq^{vM}}}_{(1)_r}(\boldsymbol{\sigma})P(\boldsymbol{\sigma},t)\right]] \\ &+\ \frac{\partial^2}{\partial\sigma_r\partial\sigma_s}\left[N^{\sigma^{eq^{vM}}}_{(2)_{rs}}(\boldsymbol{\sigma},t)P(\boldsymbol{\sigma},t)\right] \end{aligned} \tag{11}$$

where $\boldsymbol{\sigma}=\{\sigma_1,\sigma_2,\sigma_3\}$ and the indices, r and s, vary from 1 to 3. Note that for the triaxial text, σ_2 = σ_3. Therefore, (11) simplifies to a bivariate equation:

$$\frac{\partial P(\boldsymbol{\sigma},t)}{\partial t} = -P(\boldsymbol{\sigma},t)\frac{\partial N^{\sigma^{eq^{vM}}}_{(1)_1}(\boldsymbol{\sigma})}{\partial \sigma_1} - N^{\sigma^{eq^{vM}}}_{(1)_1}(\boldsymbol{\sigma})\frac{\partial P(\boldsymbol{\sigma},t)}{\partial \sigma_1}$$
$$- \quad P(\boldsymbol{\sigma},t)\frac{\partial N^{\sigma^{eq^{vM}}}_{(1)_2}(\boldsymbol{\sigma})}{\partial \sigma_2} - N^{\sigma^{eq^{vM}}}_{(1)_2}(\boldsymbol{\sigma})\frac{\partial P(\boldsymbol{\sigma},t)}{\partial \sigma_2}$$
$$+ \quad N^{\sigma^{eq^{vM}}}_{(2)_{11}}(\boldsymbol{\sigma},t)\frac{\partial^2 P(\boldsymbol{\sigma},t)}{\partial \sigma_1^2} + P(\boldsymbol{\sigma},t)\frac{\partial^2 N^{\sigma^{eq^{vM}}}_{(2)_{11}}(\boldsymbol{\sigma},t)}{\partial \sigma_1^2}$$
$$+ \quad 2\frac{\partial N^{\sigma^{eq^{vM}}}_{(2)_{11}}(\boldsymbol{\sigma},t)}{\partial \sigma_1}\frac{\partial P(\boldsymbol{\sigma},t)}{\partial \sigma_1} + N^{\sigma^{eq^{vM}}}_{(2)_{22}}(\boldsymbol{\sigma},t)\frac{\partial^2 P(\boldsymbol{\sigma},t)}{\partial \sigma_2^2}$$
$$+ \quad P(\boldsymbol{\sigma},t)\frac{\partial^2 N^{\sigma^{eq^{vM}}}_{(2)_{22}}(\boldsymbol{\sigma},t)}{\partial \sigma_2^2} + 2\frac{\partial N^{\sigma^{eq^{vM}}}_{(2)_{22}}(\boldsymbol{\sigma},t)}{\partial \sigma_2}\frac{\partial P(\boldsymbol{\sigma},t)}{\partial \sigma_2}$$
$$+ \quad 2N^{\sigma^{eq^{vM}}}_{(2)_{12}}(\boldsymbol{\sigma},t)\frac{\partial^2 P(\boldsymbol{\sigma},t)}{\partial \sigma_1 \partial \sigma_2} + 2\frac{\partial N^{\sigma^{eq^{vM}}}_{(2)_{12}}(\boldsymbol{\sigma},t)}{\partial \sigma_1}\frac{\partial P(\boldsymbol{\sigma},t)}{\partial \sigma_2}$$
$$+ \quad 2\frac{\partial N^{\sigma^{eq^{vM}}}_{(2)_{12}}(\boldsymbol{\sigma},t)}{\partial \sigma_2}\frac{\partial P(\boldsymbol{\sigma},t)}{\partial \sigma_1} + 2P(\boldsymbol{\sigma},t)\frac{\partial^2 N^{\sigma^{eq^{vM}}}_{(2)_{12}}(\boldsymbol{\sigma},t)}{\partial \sigma_1 \partial \sigma_2} \tag{12}$$

where $\boldsymbol{\sigma} = \{\sigma_1, \sigma_2\}$. By specializing (2) and (3) to the 2D principal space and applying the no volume change constraint, the elastic coefficients take the following forms:

$$\begin{aligned} N^{\sigma^{el}}_{(1)_1} &= \left\langle \frac{E}{1+\nu} \right\rangle \dot{\epsilon}_1 \\ N^{\sigma^{el}}_{(1)_2} &= -\frac{1}{2}\left\langle \frac{E}{1+\nu} \right\rangle \dot{\epsilon}_1 \\ N^{\sigma^{el}}_{(2)_{11}} &= t\ Var\left[\frac{E}{1+\nu}\right]\dot{\epsilon}_1^2 \\ N^{\sigma^{el}}_{(2)_{22}} &= t\ \frac{1}{4}Var\left[\frac{E}{1+\nu}\right]\dot{\epsilon}_1^2 \\ N^{\sigma^{el}}_{(2)_{12}} &= t\ Cov\left[\frac{E}{1+\nu}; -\frac{1}{2}\frac{E}{1+\nu}\right]\dot{\epsilon}_1^2 \end{aligned} \tag{13}$$

For a von Mises elastic-perfectly plastic soil with a yield criteria, F=$\sqrt{3J_2}-\sigma_y = 0$, where $\sqrt{J_2}$ is the second invariant of the stress tensor, the equivalent advection and diffusion coefficients can be obtained as:

$$\begin{aligned} N^{\sigma^{eq^{vM}}}_{(1)_1}(\boldsymbol{\sigma}) &= Pr[F<0](\boldsymbol{\sigma})N^{\sigma^{el}}_{(1)_1} \\ &+ \{1-Pr[F<0]\}(\boldsymbol{\sigma})N^{\sigma^{pl^{vM}}}_{(1)_1}(\boldsymbol{\sigma},t) \\ &= \left\{1-Pr[\sigma_y \le \sqrt{3J_2}]\right\}N^{\sigma^{el}}_{(1)_1} \\ N^{\sigma^{eq^{vM}}}_{(1)_2}(\boldsymbol{\sigma}) &= Pr[F<0](\boldsymbol{\sigma})N^{\sigma^{el}}_{(1)_2} \\ &+ \{1-Pr[F<0]\}(\boldsymbol{\sigma})N^{\sigma^{pl^{vM}}}_{(1)_2}(\boldsymbol{\sigma},t) \\ &= \left\{1-Pr[\sigma_y \le \sqrt{3J_2}]\right\}N^{\sigma^{el}}_{(1)_2} \end{aligned} \tag{14}$$

Note that the for a elastic-perfectly plastic model, the plastic coefficients are zero.

$$\begin{aligned} N^{\sigma^{eq^{vM}}}_{(2)_{11}}(\boldsymbol{\sigma},t) &= Pr[F<0](\boldsymbol{\sigma})N^{\sigma^{el}}_{(2)_{11}}(t) \\ &+ \{1-Pr[F<0]\}(\boldsymbol{\sigma})N^{\sigma^{pl^{vM}}}_{(2)_{11}}(\boldsymbol{\sigma},t) \\ &= \left\{1-Pr[\sigma_y \le \sqrt{3J_2}]\right\}N^{\sigma^{el}}_{(2)_{11}}(t) \\ N^{\sigma^{eq^{vM}}}_{(2)_{22}}(\boldsymbol{\sigma},t) &= Pr[F<0](\boldsymbol{\sigma})N^{\sigma^{el}}_{(2)_{22}}(t) \\ &+ \{1-Pr[F<0]\}(\boldsymbol{\sigma})N^{\sigma^{pl^{vM}}}_{(2)_{22}}(\boldsymbol{\sigma},t) \\ &= \left\{1-Pr[\sigma_y \le \sqrt{3J_2}]\right\}N^{\sigma^{el}}_{(2)_{22}}(t) \\ N^{\sigma^{eq^{vM}}}_{(2)_{12}}(\boldsymbol{\sigma},t) &= Pr[F<0](\boldsymbol{\sigma})N^{\sigma^{el}}_{(2)_{12}}(t) \\ &+ \{1-Pr[F<0]\}(\boldsymbol{\sigma})N^{\sigma^{pl^{vM}}}_{(2)_{12}}(\boldsymbol{\sigma},t) \\ &= \left\{1-Pr[\sigma_y \le \sqrt{3J_2}]\right\}N^{\sigma^{el}}_{(2)_{12}}(t) \end{aligned} \tag{15}$$

IV. Solution Algorithms

In this section, Fourier spectral approach is utilized for solving the multivariate form of the obtained FPK PDE. To use the Fourier spectral approach, the change of variable theorem is used to write (12) in terms of $\bar{\boldsymbol{\sigma}}$ which varies from 0 to 2π:

$$\frac{\partial P(\bar{\boldsymbol{\sigma}},t)}{\partial t} = -P(\bar{\boldsymbol{\sigma}},t)\frac{\partial N^{\sigma^{eq^{vM}}}_{(1)_1}(\boldsymbol{\sigma})}{\partial \bar{\sigma}_1} -$$
$$N^{\sigma^{eq^{vM}}}_{(1)_1}(\boldsymbol{\sigma})\frac{2\pi}{b_1-a_1}\frac{\partial P(\bar{\boldsymbol{\sigma}},t)}{\partial \sigma_1} - P(\bar{\boldsymbol{\sigma}},t)\frac{\partial N^{\sigma^{eq^{vM}}}_{(1)_2}(\boldsymbol{\sigma})}{\partial \sigma_2} -$$
$$N^{\sigma^{eq^{vM}}}_{(1)_2}(\boldsymbol{\sigma})\frac{2\pi}{b_2-a_2}\frac{\partial P(\bar{\boldsymbol{\sigma}},t)}{\partial \bar{\sigma}_2} +$$
$$N^{\sigma^{eq^{vM}}}_{(2)_{11}}(\boldsymbol{\sigma},t)\left(\frac{2\pi}{b_1-a_1}\right)^2\frac{\partial^2 P(\bar{\boldsymbol{\sigma}},t)}{\partial \bar{\sigma}_1^2} +$$
$$P(\bar{\boldsymbol{\sigma}},t)\frac{\partial^2 N^{\sigma^{eq^{vM}}}_{(2)_{11}}(\boldsymbol{\sigma},t)}{\partial \sigma_1^2} +$$
$$2\frac{\partial N^{\sigma^{eq^{vM}}}_{(2)_{11}}(\boldsymbol{\sigma},t)}{\partial \sigma_1}\frac{2\pi}{b_1-a_1}\frac{\partial P(\bar{\boldsymbol{\sigma}},t)}{\partial \bar{\sigma}_1} +$$
$$N^{\sigma^{eq^{vM}}}_{(2)_{22}}(\boldsymbol{\sigma},t)\left(\frac{2\pi}{b_2-a_2}\right)^2\frac{\partial^2 P(\bar{\boldsymbol{\sigma}},t)}{\partial \bar{\sigma}_2^2} +$$
$$P(\bar{\boldsymbol{\sigma}},t)\frac{\partial^2 N^{\sigma^{eq^{vM}}}_{(2)_{22}}(\boldsymbol{\sigma},t)}{\partial \sigma_2^2} +$$
$$2\frac{\partial N^{\sigma^{eq^{vM}}}_{(2)_{22}}(\boldsymbol{\sigma},t)}{\partial \sigma_2}\frac{2\pi}{b_2-a_2}\frac{\partial P(\bar{\boldsymbol{\sigma}},t)}{\partial \bar{\sigma}_2} +$$
$$2N^{\sigma^{eq^{vM}}}_{(2)_{12}}(\boldsymbol{\sigma},t)\frac{2\pi}{b_1-a_1}\frac{2\pi}{b_2-a_2}\frac{\partial^2 P(\bar{\boldsymbol{\sigma}},t)}{\partial \bar{\sigma}_1 \partial \bar{\sigma}_2} +$$
$$2\frac{\partial N^{\sigma^{eq^{vM}}}_{(2)_{12}}(\boldsymbol{\sigma},t)}{\partial \sigma_1}\frac{2\pi}{b_2-a_2}\frac{\partial P(\bar{\boldsymbol{\sigma}},t)}{\partial \bar{\sigma}_2} +$$
$$2\frac{\partial N^{\sigma^{eq^{vM}}}_{(2)_{12}}(\boldsymbol{\sigma},t)}{\partial \sigma_2}\frac{2\pi}{b_1-a_1}\frac{\partial P(\bar{\boldsymbol{\sigma}},t)}{\partial \bar{\sigma}_1} +$$
$$2P(\bar{\boldsymbol{\sigma}},t)\frac{\partial^2 N^{\sigma^{eq^{vM}}}_{(2)_{12}}(\boldsymbol{\sigma},t)}{\partial \sigma_1 \partial \sigma_2} \tag{16}$$

Using Fourier spectral approach, solution of (16) can be written in the following form:

$$P(\bar{\sigma}_1,\bar{\sigma}_2,t)=\sum_{n=-\frac{N}{2}}^{\frac{N}{2}}\sum_{m=-\frac{M}{2}}^{\frac{M}{2}}\alpha_{mn}(t)e^{i(n\bar{\sigma}_1+m\bar{\sigma}_2)} \tag{17}$$

where $i=\sqrt{-1}$, and $\alpha_{mn}(t)$ is the unknown time-dependent coefficients. By substituting (17) into (16), a system of ordinary differential equations may be obtained:

$$\begin{aligned}
&\sum_{n=-\frac{N}{2}}^{\frac{N}{2}}\sum_{m=-\frac{M}{2}}^{\frac{M}{2}}\Big[\alpha'_{mn}(t)+\langle\lambda\rangle\,\dot{\epsilon}_1\left\{1-Pr\left[\sigma_y\le\sqrt{3J_2}\right]\right\}\\
&\left(\frac{2\pi}{b_1-a_1}\right)in\,\alpha_{mn}(t)+\\
&\langle\lambda\rangle\,\dot{\epsilon}_1\frac{\partial}{\partial\sigma_1}\left\{1-Pr\left[\sigma_y\le\sqrt{3J_2}\right]\right\}\alpha_{mn}(t)+\left\langle-\frac{1}{2}\lambda\right\rangle\\
&\dot{\epsilon}_1\left\{1-Pr\left[\sigma_y\le\sqrt{3J_2}\right]\right\}\left(\frac{2\pi}{b_2-a_2}\right)im\,\alpha_{mn}(t)+\\
&\left\langle-\frac{1}{2}\lambda\right\rangle\dot{\epsilon}_1\frac{\partial}{\partial\sigma_2}\left\{1-Pr\left[\sigma_y\le\sqrt{3J_2}\right]\right\}\alpha_{mn}(t)-\\
&t\,\alpha_{mn}(t)\left\{Var\left[\lambda\right]\dot{\epsilon}_1^2\left\{1-Pr\left[\sigma_y\le\sqrt{3J_2}\right]\right\}\right.\\
&\left(\frac{2\pi}{b_1-a_1}\right)^2n^2+2\left(\frac{2\pi}{b_1-a_1}\right)Var\left[\lambda\right]\dot{\epsilon}_1^2\\
&\frac{\partial}{\partial\sigma_1}\left\{1-Pr\left[\sigma_y\le\sqrt{3J_2}\right]\right\}in\;+Var\left[\lambda\right]\dot{\epsilon}_1^2+\\
&\frac{\partial^2}{\partial\sigma_1^2}\left\{1-Pr\left[\sigma_y\le\sqrt{3J_2}\right]\right\}Var\left[-\frac{1}{2}\lambda\right]\dot{\epsilon}_1^2\\
&\left\{1-Pr\left[\sigma_y\le\sqrt{3J_2}\right]\right\}\left(\frac{2\pi}{b_2-a_2}\right)^2m^2+\\
&2\left(\frac{2\pi}{b_2-a_2}\right)Var\left[-\frac{1}{2}\lambda\right]\dot{\epsilon}_1^2\frac{\partial}{\partial\sigma_2}\\
&\left\{1-Pr\left[\sigma_y\le\sqrt{3J_2}\right]\right\}im\;+Var\left[-\frac{1}{2}\lambda\right]\dot{\epsilon}_1^2+\\
&\frac{\partial^2}{\partial\sigma_2^2}\left\{1-Pr\left[\sigma_y\le\sqrt{3J_2}\right]\right\}2Cov\left[\lambda;-\frac{1}{2}\lambda\right]\dot{\epsilon}_1^2\\
&\left\{1-Pr\left[\sigma_y\le\sqrt{3J_2}\right]\right\}\left(\frac{2\pi}{b_1-a_1}\right)\left(\frac{2\pi}{b_2-a_2}\right)nm\\
&+2\left(\frac{2\pi}{b_2-a_2}\right)Cov\left[\lambda;-\frac{1}{2}\lambda\right]\dot{\epsilon}_1^2\\
&\frac{\partial}{\partial\sigma_1}\left\{1-Pr\left[\sigma_y\le\sqrt{3J_2}\right]\right\}im+2\left(\frac{2\pi}{b_1-a_1}\right)\\
&Cov\left[\lambda;-\frac{1}{2}\lambda\right]\dot{\epsilon}_1^2\frac{\partial}{\partial\sigma_2}\left\{1-Pr\left[\sigma_y\le\sqrt{3J_2}\right]\right\}in+\\
&2Cov\left[\lambda;-\frac{1}{2}\lambda\right]\dot{\epsilon}_1^2\\
&\left.\left.\frac{\partial^2}{\partial\sigma_1\partial\sigma_2}\left\{1-Pr\left[\sigma_y\le\sqrt{3J_2}\right]\right\}\right\}\right]e^{i(n\bar{\sigma}_1+m\bar{\sigma}_2)}=0
\end{aligned} \tag{18}$$

where $\lambda=E/(1+\nu)$. Note that in the above equation, the coefficients, $N^{\sigma^{el}}_{(1)_1}$, $N^{\sigma^{el}}_{(1)_2}$, $N^{\sigma^{el}}_{(2)_{11}}$, $N^{\sigma^{el}}_{(2)_{22}}$, and $N^{\sigma^{el}}_{(2)_{12}}$, are substituted by their definitions (refer to (13), (14) and (15)). Finally, employing the Euler method, (18) may be solved for the unknown coefficients, α_{mn}, at $t=t_{j+1}$ given the coefficients at $t=t_j$:

$$\begin{aligned}
&\alpha_{mn}(t_{j+1})=\alpha_{mn}(t_j)-\Delta t\\
&\Big[\langle\lambda\rangle\,\dot{\epsilon}_1\left\{1-Pr\left[\sigma_y\le\sqrt{3J_2}\right]\right\}\left(\frac{2\pi}{b_1-a_1}\right)in\\
&+\alpha_{mn}(t_j)\,\langle\lambda\rangle\,\dot{\epsilon}_1\frac{\partial}{\partial\sigma_1}\left\{1-Pr\left[\sigma_y\le\sqrt{3J_2}\right]\right\}\alpha_{mn}(t_j)\\
&+\left\langle-\frac{1}{2}\lambda\right\rangle\dot{\epsilon}_1\left\{1-Pr\left[\sigma_y\le\sqrt{3J_2}\right]\right\}\left(\frac{2\pi}{b_2-a_2}\right)\\
&im\,\alpha_{mn}(t_j)+\left\langle-\frac{1}{2}\lambda\right\rangle\dot{\epsilon}_1\frac{\partial}{\partial\sigma_2}\left\{1-Pr\left[\sigma_y\le\sqrt{3J_2}\right]\right\}\\
&\alpha_{mn}(t_j)-t_{j+1}\,\alpha_{mn}(t_j)\left\{Var\left[\lambda\right]\dot{\epsilon}_1^2\right.\\
&\left\{1-Pr\left[\sigma_y\le\sqrt{3J_2}\right]\right\}\left(\frac{2\pi}{b_1-a_1}\right)^2n^2+\\
&2\left(\frac{2\pi}{b_1-a_1}\right)Var\left[\lambda\right]\dot{\epsilon}_1^2\frac{\partial}{\partial\sigma_1}\left\{1-Pr\left[\sigma_y\le\sqrt{3J_2}\right]\right\}\\
&in+Var\left[\lambda\right]\dot{\epsilon}_1^2\frac{\partial^2}{\partial\sigma_1^2}\left\{1-Pr\left[\sigma_y\le\sqrt{3J_2}\right]\right\}+\\
&Var\left[-\frac{1}{2}\lambda\right]\dot{\epsilon}_1^2\left\{1-Pr\left[\sigma_y\le\sqrt{3J_2}\right]\right\}\left(\frac{2\pi}{b_2-a_2}\right)^2\\
&m^2+2\left(\frac{2\pi}{b_2-a_2}\right)Var\left[-\frac{1}{2}\lambda\right]\dot{\epsilon}_1^2\frac{\partial}{\partial\sigma_2}\\
&\left\{1-Pr\left[\sigma_y\le\sqrt{3J_2}\right]\right\}im\;+\\
&Var\left[-\frac{1}{2}\lambda\right]\dot{\epsilon}_1^2\frac{\partial^2}{\partial\sigma_2^2}\left\{1-Pr\left[\sigma_y\le\sqrt{3J_2}\right]\right\}+\\
&2Cov\left[\lambda;-\frac{1}{2}\lambda\right]\dot{\epsilon}_1^2\left\{1-Pr\left[\sigma_y\le\sqrt{3J_2}\right]\right\}\left(\frac{2\pi}{b_1-a_1}\right)\\
&\left(\frac{2\pi}{b_2-a_2}\right)nm+2\left(\frac{2\pi}{b_2-a_2}\right)Cov\left[\lambda;-\frac{1}{2}\lambda\right]\dot{\epsilon}_1^2\\
&\frac{\partial}{\partial\sigma_1}\left\{1-Pr\left[\sigma_y\le\sqrt{3J_2}\right]\right\}im+2\left(\frac{2\pi}{b_1-a_1}\right)\\
&Cov\left[\lambda;-\frac{1}{2}\lambda\right]\dot{\epsilon}_1^2\frac{\partial}{\partial\sigma_2}\left\{1-Pr\left[\sigma_y\le\sqrt{3J_2}\right]\right\}in+\\
&\left.2Cov\left[\lambda;-\frac{1}{2}\lambda\right]\dot{\epsilon}_1^2\frac{\partial^2}{\partial\sigma_1\partial\sigma_2}\left\{1-Pr\left[\sigma_y\le\sqrt{3J_2}\right]\right\}\right\}\Big]
\end{aligned} \tag{19}$$

Note that at $t=t_0$, the coefficients, $\alpha_{mn}(t_0)$ may be obtained from the initial condition, $P(\bar{\sigma}_{l_1},\bar{\sigma}_{l_2},t_0)$ as:

$$\begin{aligned}
&\sum_{n=-\frac{N}{2}}^{\frac{N}{2}}\sum_{m=-\frac{M}{2}}^{\frac{M}{2}}\alpha_{mn}(t_0)e^{i(n\bar{\sigma}_{l_1}+m\bar{\sigma}_{l_2})}=P(\bar{\sigma}_{l_1},\bar{\sigma}_{l_2},t_0)\\
&\text{or,}\quad \alpha_{mn}(t_0)=\\
&\frac{1}{N+1}\frac{1}{M+1}\sum_{l_1=0}^{N}\sum_{l_2=0}^{M}P(\bar{\sigma}_{l_1},\bar{\sigma}_{l_2},t_0)\,e^{-i(n\bar{\sigma}_{l_1}+m\bar{\sigma}_{l_2})}
\end{aligned} \tag{20}$$

where $\bar{\sigma}_{l_1}=\frac{2\pi}{N}l_1$, $\bar{\sigma}_{l_2}=\frac{2\pi}{M}l_2$, and $l_1=0,1,2,\cdots,N$, and $l_2=0,1,2,\cdots,M$. Equation (19) may then be used to

increment the solution forward in time.

V. Results and Discussion

The above presented algorithm for solving the FPK PDE is implemented using the programming language C++. The codes are publicly available through the corresponding author's website. Simulation results are presented in this section in terms of probabilistic constitutive responses of von Mises elastic-perfectly plastic soils under unconsolidated undrained cyclic triaxial compression test.

To model cyclic behavior of soils, one hysteresis loop which consists of three branches (loading, unloading and reloading) is simulated. The loading branch is similar to the monotonic simulation and can be found up to 1% strain by solving (12). Note that, in the cyclic simulation, $Pr\left[\sigma_y \leq \sqrt{3J_2}\right]$ in (19) should be replaced by $Pr\left[\sigma_y^2 \leq 3J_2\right]$. In this simulation, σ_y is considered to be a Weibull random variable and correspondingly the J_2-dependent probabilities appearing in (19) were computed as:

$$Pr\left[\sigma_y^2 \leq 3J_2\right] = CDF\left[\text{Weibull Distribution}\left[\theta,\kappa\right],3J_2\right] = \begin{cases} 1-e^{-\left(\frac{3J_2}{\theta}\right)^{\kappa}} & \text{when } (\sigma_1-\sigma_2)\geq 0 \\ 0 & \text{when } (\sigma_1-\sigma_2)<0 \end{cases} \quad (21)$$

Note that, $3J_2 = (\sigma_1-\sigma_2)^2$, θ and κ are the parameters of the Weibull distribution. They were obtained from the mean and variance of yield stress using the following relationships [28]:

$$\theta\Gamma\left(1+\frac{1}{\kappa}\right) = \langle\sigma_y\rangle\,\theta^2\left[\Gamma\left(1+\frac{2}{\kappa}\right)-\left\{\Gamma\left(1+\frac{1}{\kappa}\right)\right\}^2\right] = \text{Var}\left[\sigma_y\right] \quad (22)$$

where $\Gamma(\cdot)$ denotes the gamma function.

Similarly, the unloading branch can be obtained up to -1% strain by solving (12); however, in computing $N_{(1)_r}^{\sigma^{eq^{vM}}}(\sigma)$ and $N_{(2)_r}^{\sigma^{eq^{vM}}}$, $\dot{\epsilon}_1$ should be replaced by $-\dot{\epsilon}_1$. Moreover, the J_2-dependent probabilities appearing in (19) were computed as:

$$Pr\left[\sigma_y^2 \leq 3J_2\right] = CDF\left[\text{Weibull Distribution}\left[\theta,\kappa\right],3J_2\right] = \begin{cases} 1-e^{-\left(\frac{3J_2}{\theta}\right)^{\kappa}} & \text{when } (-\sigma_1+\sigma_2)\geq 0 \\ 0 & \text{when } (-\sigma_1+\sigma_2)<0 \end{cases} \quad (23)$$

Finally, the reloading branch is obtained up to 1% strain by solving (12) with the same coefficients as the loading simulation. It should be mentioned that the initial condition of the unloading branch is the solution of the loading branch at the 1% strain, and the initial condition of the reloading branch is the solution of unloading branch at -1% strain.

In this simulation, the Young's modulus, E, of the soil is assumed to be a normal random variable with a mean value of 100 MPa and a coefficient of variation (COV) of 20%. On the other hand, the yield stress, σ_y, is assumed to be a Weibull random variable with a mean value of 150 kPa and a COV of 50%.

The simulation result is obtained in terms of the evolutionary joint PDF of the axial and radial stresses. The marginal PDFs of the axial and radial stresses can be computed by using the standard integration techniques. Note that all the results presented below are processed through a Kaiser window to minimize spurious oscillations in the solutions.

Figs. 1 and 2 show the evolutionary marginal PDFs of the axial and radial stresses, which include all the information on the statistical moments of the stresses, such as the evolutionary mean and standard deviation, at the end of loading, unloading and reloading.

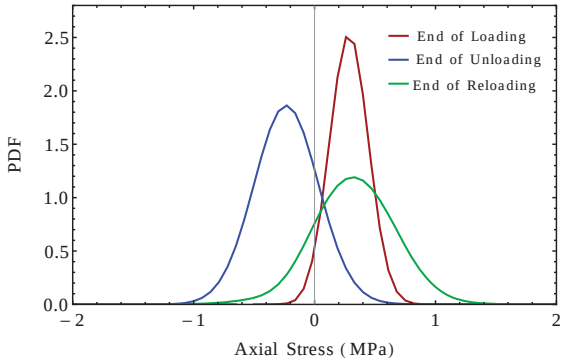

Fig. 1 Probability density function (PDF) of the axial stress for an uncertain von Mises cyclic elastic–perfectly plastic soil under an unconfined compression test

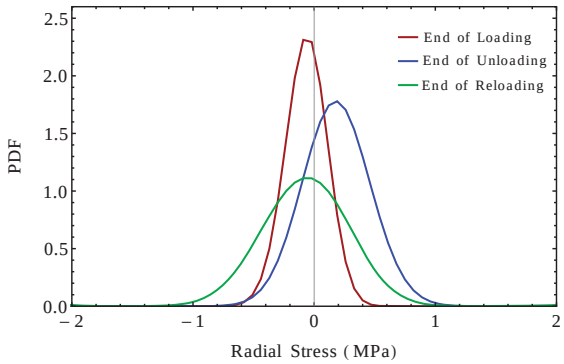

Fig. 2 Simulated probabilistic cyclic elastic–perfectly plastic behavior in terms of the evolutionary mean of deviatoric stress with axial strain

Typical cyclic undrained responses are also obtained in terms of the evolutionary mean and standard deviation of deviatoric stress, $q = \sigma_1 - \sigma_2$, with axial strain (ϵ_a), and deviatoric stress (q) with mean effective stress, $p' = \frac{1}{3}(\sigma_1 + 2\sigma_2)$, by post–processing the evolutionary joint PDF of the stresses (Figs. 3-5) [2].

As can be seen in Fig. 3, the mean stress is nonlinear even at very small strain. This is due to the uncertainty in the yield strength which means that there is always a chance that soil plastifies at a very small strain. Moreover,

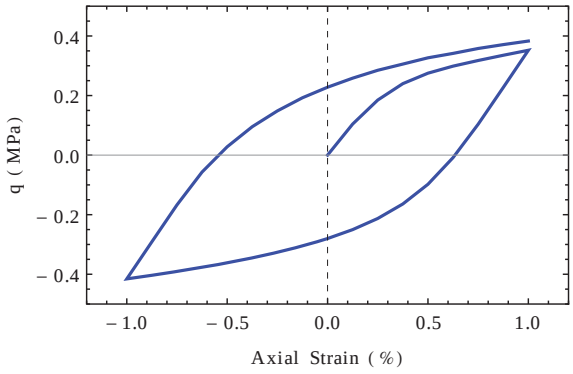

Fig. 3 Effect of the number of Fourier terms on the simulated evolutionary mean and standard deviation behaviors of the axial stress with the axial strain for an uncertain von Mises elastic-perfectly plastic soil under an unconfined compression test

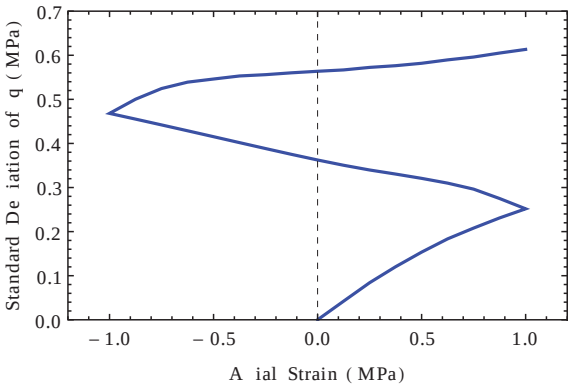

Fig. 4 Simulated probabilistic cyclic elastic–perfectly plastic behavior in terms of the evolutionary standard deviation of deviatoric stress with axial strain

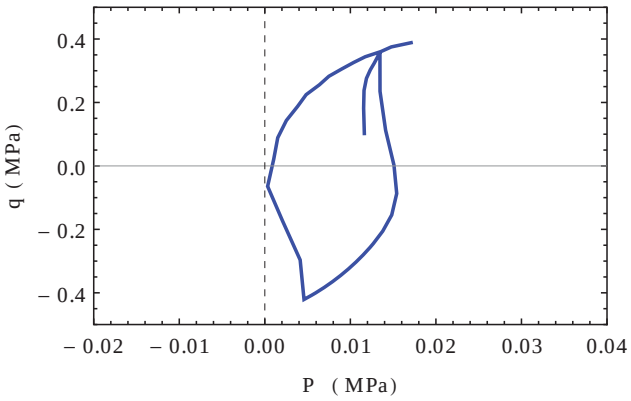

Fig. 5 Simulated probabilistic cyclic elastic–perfectly plastic behavior in terms of the evolutionary mean of deviatoric stress with evolutionary mean effective stress

it is possible that soil remains elastic at strains past the yield point. Therefore, the mean solution can be explained as the ensemble average of all the possibilities. This agrees well with the soil behavior that is usually observed in any laboratory experiment. In general, within a laboratory specimen (considered as representative volume element [29]) each particle contacts has different yield strength and the observed soil behavior in the experiment is the ensemble average (mean) behavior of all the particle contacts. This figure also shows that by considering the uncertainties in material properties, the hardening and Bauschinger effect can also be captured even with a simple von Mises elastic–perfectly plastic (two–parameters) model. On the other hand, Fig. 4 shows the evolutionary standard deviation behavior obtained by post–processing the evolutionary PDF of the stress. It is important to note that the standard deviation behavior depends on the soil parameters, and by using a different values of COV for elastic modulus (E) or yield strength (σ_y), a totally different behavior may be observed. In general, when the material is elastic, both the uncertainties in elastic modulus (E) and yield strength (σ_y) are governing. However, as soil becomes elastic–plastic, the influence of uncertainty in elastic modulus (E) decreases, and the uncertainty in yield strength is governing. This figure also shows that the standard deviation always increases. This indicates that as material plastifies, the two–parameter von Mises elastic–perfectly plastic becomes less and less accurate. Therefore, in order to get more accurate results, more advanced constitutive (isotropic/kinematic hardening) models are required. Note that this behavior is not generic, and it depends on the material parameters. The evolutionary effective stress path is also shown in Fig. 5.

Note that the evolutionary statistics were computed by integrating the solutions – probability density function and joint probability density function – after each (pseudo) time step using standard techniques. It also should be mentioned that the presented solutions were obtained using sixty Fourier terms in each direction. In this context, it is important to emphasize that, the presented hybrid spectral-finite difference algorithm is conditionally stable – the product of the number of Fourier terms and (pseudo) time step-size (Δt) should be less than 2. Based on the simulations performed in this study, a value between 0.2 and 2 is recommended for optimum efficiency and stability.

VI. Conclusion

In this study the existing one dimensional FPK framework for probabilistic cyclic constitutive modeling of soils was extended to multi-dimension. The developed algorithms were then used to probabilistically simulate the multiaxial cyclic constitutive behaviors of uncertain elasto-plastic soils. In particular, the unconsolidated undrained triaxial compression test (common laboratory constitutive experiments in geotechnical engineering) was considered.

The elastic-perfectly plastic cyclic unconsolidated undrained triaxial compression simulation results indicated that, even with the elastic-perfectly plastic (i.e, bilinear) model, due to uncertainty in yielding, the probabilistic response was smooth and nonlinear from the beginning. This response is very realistic and it means that depending upon the uncertainty in yield strength, there is always a possibility that the soil

becomes elastic-plastic from the very beginning of loading, which agrees well with the fact that within a representative volume element of a spatially non-uniform material like soils some particle-to-particle slips may occur earlier than others.

It was also shown that explicit treatment of soil uncertainties not only allows for quantification of our confidence in our predictions, but also modeling some of the important aspects of soil behaviors-for example, hardening and Bauschinger effect-even with the simplest elastic-perfectly plastic von Mises (two-parameters) model. This is particularly significant since in geotechnical engineering practice, advanced laboratory tests are rarely performed.

Acknowledgment

The work presented in this paper was supported in part by a grant from the Civil, Mechanical and Manufacturing Innovation program of the Directorate of Engineering of the National Science Foundation under award # NSF–CMMI–1200196 (cognizant program director: Dr. Richard Fragaszy).

References

[1] A. N. Schofield and P. Wroth, *Critical state soil mechanics*. McGraw-Hill, 1968, (Reissued by Dover Publications, 2003).

[2] Y. F. Dafalias and M. T. Manzari, "Simple plasticity sand model accounting for fabric change effects," *ASCE Journal of Engineering Mechanics*, vol. 130, no. 6, pp. 622–634, June 2004.

[3] A. Vytiniotis, "Contributions to the analysis and mitigation of liquefaction in loose sand slopes," Doctoral Dissertation, Massachusetts Institute of Technology, Boston, MA, September 2011.

[4] R. W. Boulanger and K. Ziotopoulou, "Formulation of a sand plasticity plane-strain model for earthquake engineering applications," *Soil Dynamics and Earthquake Engineering*, vol. 53, pp. 254–267, 2013.

[5] G. A. Fenton, "Estimation of stochastic soil models," *Journal of Geotechnical and Geoenvironmental Engineering, ASCE*, vol. 125, no. 6, pp. 470–485, June 1999.

[6] D. J. DeGroot and G. B. Baecher, "Estimating autocovariance of in-situ soil properties," *Journal of Geotechnical Engineering*, vol. 119, no. 1, pp. 147–166, January 1993.

[7] G. M. Hammitt, "Statistical analysis of data from a comparative laboratory test program sponsored by ACITL," U.S. Army Waterways Experiment Station, Vicksburg, MS, 1966.

[8] K.-K. Phoon and F. H. Kulhawy, "Characterization of geotechnical variability," *Canadian Geotechnical Journal*, vol. 36, no. 4, pp. 612–624, 1999.

[9] K. T. Marosi and D. R. Hiltunen, "Characterization of spectral analysis of surface waves shear wave velocity measurement uncertainty," *Journal of Geotechnical and Geoenvironmental Engineering, ASCE*, vol. 130, no. 10, pp. 1034–1041, October 2004.

[10] S. Lacasse and F. Nadim, "Uncertainties in characterizing soil properties," in *Uncertainty in Geologic Environment: From Theory to Practice, Proceedings of Uncertainty '96, July 31-August 3, 1996, Madison, Wisconsin*, ser. Geotechnical Special Publication No. 58, C. D. Shackelford and P. P. Nelson, Eds., vol. 1. ASCE, New York, 1996, pp. 49–75.

[11] K.-K. Phoon and F. H. Kulhawy, "Evaluation of geotechnical property variability," *Canadian Geotechnical Journal*, vol. 36, no. 4, pp. 625–639, 1999.

[12] G. M. Paice, D. V. Griffiths, and G. A. Fenton, "Finite element modeling of settlement on spatially random soil," *Journal of Geotechnical Engineering*, vol. 122, no. 9, pp. 777–779, 1996.

[13] R. Popescu, J. H. Prevost, and G. Deodatis, "Effects of spatial variability on soil liquefaction: Some design recommendations," *Geotechnique*, vol. 47, no. 5, pp. 1019–1036, 1997.

[14] B. S. L. P. De Lima, E. C. Teixeira, and N. F. F. Ebecken, "Probabilistic and possibilistic methods for the elastoplastic analysis of soils," *Advances in Engineering Software*, vol. 132, pp. 569–585, 2001.

[15] S. Koutsourelakis, J. H. Prevost, and G. Deodatis, "Risk assesment of an interacting structure-soil system due to liquefaction," *Earthquake Engineering and Structural Dynamics*, vol. 31, pp. 851–879, 2002.

[16] D. V. Griffiths, G. A. Fenton, and N. Manoharan, "Bearing capacity of rough rigid strip footing on cohesive soil: Probabilistic study," *Journal of Geotechnical and Geoenvironmental Engineering, ASCE*, vol. 128, no. 9, pp. 743–755, 2002.

[17] M. Kleiber and T. D. Hien, *The Stochastic Finite Element Method: Basic Perturbation Technique and Computer Implementation*. Baffins Lane, Chichester, West Sussex PO19 1UD , England: John Wiley & Sons, 1992.

[18] B. Sudret and A. Der Kiureghian, "Stochastic finite element methods and reliability: A state of the art report," University of California, Berkeley, Technical Report UCB/SEMM-2000/08, 2000.

[19] K. Sett and B. Jeremić, "Probabilistic yielding and cyclic behavior of geomaterials," *International Journal for Numerical and Analytical Methods in Geomechanics*, vol. 34, no. 15, pp. 1541–1559, 2010.

[20] K. Sett, B. Unutmaz, K. O. Çetin, S. Koprivica, and B. Jeremić, "Soil uncertainty and its influence on simulated G/G_{max} and damping behavior," *Journal of Geotechnical and Geoenvironmental Engineering*, vol. 137, no. 3, pp. 197–204, March 2011.

[21] M. L. Kavvas, "Applied Stochastic Methods in Engineering (ECI 266) classnotes," Lecture Notes, University of California, Davis, 1993.

[22] B. Jeremić, K. Sett, and M. L. Kavvas, "Probabilistic elasto-plasticity: Formulation in 1–D," *Acta Geotechnica*, vol. 2, no. 3, pp. 197–210, September 2007.

[23] K. Sett, B. Jeremić, and M. L. Kavvas, "Probabilistic elasto-plasticity: Solution and verification in 1–D," *Acta Geotechnica*, vol. 2, no. 3, pp. 211–220, September 2007.

[24] K. Sett, B. Jeremić, and M. L. Kavvas, "The role of nonlinear hardening/softening in probabilistic elasto–plasticity," *International Journal for Numerical and Analytical Methods in Geomechanics*, vol. 31, no. 7, pp. 953–975, June 2007.

[25] B. Jeremić and K. Sett, "On probabilistic yielding of materials," *Communications in Numerical Methods in Engineering*, vol. 25, no. 3, pp. 291–300, 2009.

[26] W. F. Chen and D. J. Han, *Plasticity for Structural Engineers*. Springer-Verlag, 1988.

[27] B. M. Das, *Soil Mechanics Laboratory Manual*, 8th ed. New York, NY: Oxford University Press, 2013.

[28] D. C. Montgomery and G. C. Runger, *Applied Statistics and Probability for Engineers*, 3rd ed. 605 Third Avenue, New York, NY 10158: John Wiley & Sons, 2003.

[29] Z. Hashin, "Analysis of composite materials," *Journal of Applied Mechanics*, vol. 50, pp. 481–501, 1983.